



# Experimental verification of high-performance polymer gears in an electric vehicle powertrain

S. Reitschuster<sup>1</sup> · T. Tobie<sup>1</sup> · K. Stahl<sup>1</sup>

Received: 24 March 2023 / Accepted: 6 June 2023 / Published online: 30 June 2023  
© The Author(s) 2023

## Abstract

Gears made of polymers increasingly gain relevance in current research and industrial practice. Due to their advantages such as low density and the possibility of cost-efficient production in large quantities, more and more efforts are made to substitute steel gears with polymer wherever possible. However, the usage of polymer gears in current vehicle systems is still almost exclusively limited to applications with restricted power transmission, like actuators. To extend the field of application to power transmissions as well, in this study a transmission was developed for the usage in a small electric vehicle of the 7Le power class considering the application of polymer gears. Compared to the serial transmission, one of the gear stages was completely substituted with polymer gears. The load-carrying capacity of the newly designed hybrid polymer-steel transmission was investigated for functional verification on a specially developed test rig as well as inside a modified demonstrator vehicle under real-life conditions. Assuming usual operating conditions, the load-carrying capacity of the polymer gears appears suitable for the aimed application on the test rig as well as inside the demonstrator vehicle. Moreover, with increased power and under continuous sustained loading, high performance of the polymer stage as well as a stable temperature behavior can be observed. Under the given circumstances, polymer gears can be used as part of a powertrain in small electric vehicles.

## Experimentelle Untersuchung von Hochleistungskunststoffzahnradern im Antriebsstrang eines Elektrofahrzeugs

### Zusammenfassung

Zahnradern aus Kunststoff gewinnen in der aktuellen Forschung sowie in der industriellen Praxis zunehmend an Bedeutung. Aufgrund diverser Vorteile wie z. B. einer geringen Dichte und der Möglichkeit einer kosteneffizienten Produktion großer Stückzahlen gibt es verstärkt Bemühungen Stahlzahnradern durch Kunststoff zu ersetzen, wo immer dies möglich ist. Aktuell ist der Einsatz von Kunststoffzahnradern in viele technischen Bereichen allerdings noch immer fast ausschließlich auf Anwendungen mit begrenzter Leistungsübertragung, wie z. B. Aktuatoren, beschränkt. Um das Leistungsspektrum zu erweitern, wurde in dieser Studie ein Getriebe für den Einsatz in einem Elektrokleinstfahrzeug der Leistungsklasse 7Le entwickelt unter Berücksichtigung des Einsatzes von Kunststoffzahnradern. Im Vergleich zum Seriengeräte wurde eine der beiden Getriebestufen dabei komplett durch Kunststoffzahnradern substituiert. Die Tragfähigkeit des neu entwickelten Kunststoff-Stahl-Getriebes wurde zum Funktionsnachweis auf einem speziell entwickelten Prüfstand sowie in einem modifizierten Demonstratorfahrzeug unter realen Bedingungen untersucht. Unter der Annahme üblicher Betriebsbedingungen zeigt sich sowohl im Prüfstand als auch im Demonstratorfahrzeug eine ausreichende Tragfähigkeit des Kunststoff-Stahl-Getriebes. Darüber hinaus sind auch bei erhöhter Leistung und unter kontinuierlicher Dauerbelastung eine hohe Leistungsfähigkeit sowie ein stabiles Temperaturverhalten der Kunststoffzahnradern zu beobachten. Unter den gegebenen Rahmenbedingungen erscheint daher der Einsatz von Kunststoffzahnradern als Teil eines Antriebsstrangs in einem Elektrokleinstfahrzeug als möglich.

✉ S. Reitschuster  
stefan.reitschuster@tum.de

<sup>1</sup> Gear Research Center (FZG), Technical University of Munich (TUM), Munich, Germany

## 1 State of knowledge

Small electric vehicles designed for urban traffic applications are becoming increasingly attractive for private transportation but also for logistics services (i.e. last-mile delivery). The powertrain of such battery electric vehicles (BEV) generally consists of four elements:

- High-voltage battery pack
- Electric motor/generator
- Power inverter
- Transmission

In vehicles with conventional combustion engines, a multi-speed manual or automatic transmission is a necessary component in the powertrain. In contrast, electric vehicles theoretically can drive without torque and speed conversion due to their torque characteristics. However, to achieve sufficient driving performance with high maximum speed and simultaneously high torque from the standstill, large e-machines would be necessary, that are expensive and heavy. Therefore electric vehicles are also equipped with a transmission with a typical ratio in the range of  $i=10$ . Usually, cylindrical gear transmissions with 1- or 2-stage designs are used for this kind of application. Due to various advantages such as insensitivity to changes in center distance and broad basic knowledge almost exclusively cylindrical gears with involute profile are used for this purpose.

The calculation of the load-carrying capacity for cylindrical gears made of steel is extensively researched and documented in different standards like ISO 6336 [1]. Conversely, the knowledge base in the field of cylindrical polymer gears is still very limited, although the number of applications with polymer gears has been rising sharply in recent years [2]. While polymer gears were initially only used to transmit motion, such as in steering systems or electric actuators for seats or window lifters, high-performance polymers are now increasingly found in applications with higher power transmission, due to advantages like low weight, quiet running, and the possibility of cost-efficient manufacturing in large quantities. Even in safety-relevant applications such as electric parking brakes and electric steering systems polymer gears are integrated in the meantime [2]. Another emerging field of application of polymer gears are e-bikes with a power range up to 1 kW using the advantages of polymer to optimize the cost and weight of the powertrain. Following this trend, [3, 4] describe the design of polymer gears for an application with even higher power transmission such as in small electric vehicles. The verification of the load-carrying capacity for the polymer gears in the selected powertrain of a small electric vehicle is thereby proven based on theoretical studies. The designed hybrid polymer-steel transmission provides the basis for the

results presented in this study. However, the experimental verification of the load-carrying capacity of thermoplastic gears in applications in this power range is not yet known. In general, there is a large number of publications on the wear, damage, and temperature behavior of polymer gears [5]. However, studies of applications in a power range comparable to this one have hardly been published. According to VDI 2736 [6], polymer gears show some similar damage types as steel gears which generally can be classified as follows.

- Melting
- Tooth root breakage
- Tooth flank shear damage
- Pitting
- Wear
- Plastic deformation

Under oil-lubricated conditions melting and wear usually become negligible. In comparison with dry running, power density could be significantly increased by the lubricant [7]. Thus, relevant damage types under these conditions are tooth root breakage and damages to the tooth flank in form of breakage or pitting. Furthermore, the lubricated polymer contact can offer very low coefficients of friction in the range of superlubricity for certain lubrication conditions [8, 9]. The material-related differences between polymers and steel necessitate new or adapted calculation methods for the design of polymer gears. They are defined in VDI 2736 [10] and specifically cover the calculation of the tooth flank and tooth root load-carrying capacity. The calculation methods according to VDI 2736 [VDI14b] follow the guidelines for steel gears contained in ISO 6336 [ISO06c] and DIN 3990 [DIN 87c]. The decisive calculation parameter for the tooth flank load capacity is the occurring flank pressure  $\sigma_H$ , which can be calculated based on the Hertzian pressure theory at the pitch point. Equations 1 and 2 describe the calculation of the tooth root stress  $\sigma_F$  and the flank pressure  $\sigma_H$  according to VDI 2736 [10].

$$\sigma_H = Z_E \cdot Z_H \cdot Z_\varepsilon \cdot Z_\beta \cdot \sqrt{\frac{F_t \cdot K_H}{b_w \cdot d_1} \cdot \frac{u+1}{u}} \quad (1)$$

$$\sigma_F = K_F \cdot Y_{Fa} \cdot Y_{Sa} \cdot Y_\varepsilon \cdot Y_\beta \cdot \frac{F_t}{b \cdot m_n} \quad (2)$$

For the evaluation of the load-carrying capacity, the calculated stress is compared to the permissible stress, which is based on the strength, derived for each material and temperature from experimentally determined S/N curves. However, the use of this approach is restricted by the fact that in VDI 2736 [10] corresponding strength values are currently only available for a very limited number of polymer and

conditions. Furthermore, not all relevant influences on the load-carrying capacity of polymer gears are fully covered so far.

As shown in [11, 12], the tooth root stresses calculated according to VDI 2736 [10] provide values that are too high. The reason for this is the inadequate consideration of tooth deformation under load, which can lead to a significant increase in contact ratio and thus can have a positive effect on the load sharing between several teeth and the load distribution in the tooth contact. In addition, the high tooth deformation can also lead to premature and posterior tooth meshing, which can result in significant pressure peaks on the tooth flank either not considered in the calculations of VDI 2736 [10].

## 2 Aim of this work

Polymer gears increasingly gain importance also in applications with higher power requirements. In preliminary studies [4], a polymer-steel transmission demonstrator was designed for the use in the powertrain of a small electric vehicle, considering the specific material properties of thermoplastic gears. The present work is about the investigation of the load-carrying capacity of thermoplastic gears under close-to-reality conditions in a specially designed test rig as well as in a demonstrator vehicle.

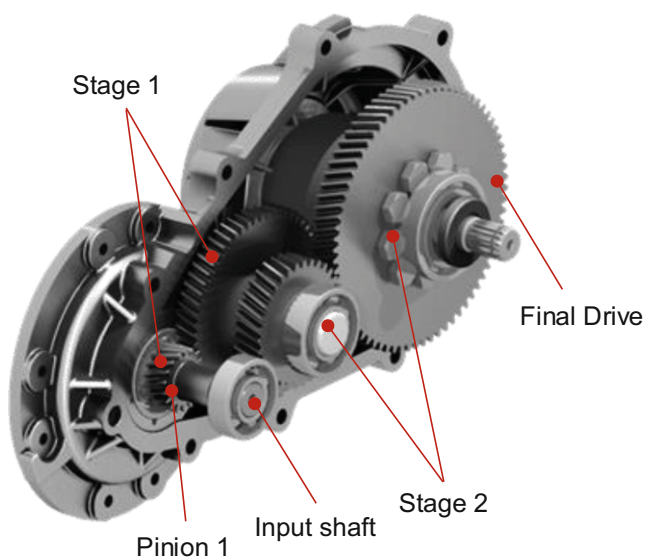


**Fig. 1** Schematic illustration of the serial transmission of the Renault Twizy

## 3 Serial test vehicle

The designed transmission demonstrator consists of polymer and steel gears and is investigated in a small electric vehicle, the Renault Twizy classified as a light vehicle L7e. Vehicles in this class are limited to a maximum empty mass of  $m_{\text{empty}} = 450 \text{ kg}$  and a maximum drive power of  $P_{\text{max}} = 15 \text{ kW}$ . The main technical data of the demonstrator vehicle Renault Twizy are summarized below:

- Powertrain: electric
- Constant power  $P_{\text{constant}}$ : 8 kW
- Peak power  $P_{\text{peak}}$ : 13 kW (for some seconds)
- Maximum torque  $T_{\text{max}}$ : 57 Nm
- Maximum speed  $v_{\text{max}}$ : 80 km/h
- Acceleration 0–50 km/h: 7 s

The serial transmission used in the Renault Twizy is a non-shiftable 2-stage spur gear transmission made entirely of steel materials. Figure 1 shows the components of the serial transmission schematically in the open state. Torque is transmitted from the electric machine to the steel pinion via the input shaft before being transferred to the rear wheels via two spur gear stages. Gear stage 1 and 2 consist of two cylindrical gears each with teeth numbers of  $z_{11} = 14$  and  $z_{12} = 61$  ( $i_1 = 4.36$ ) in stage 1 and  $z_{21} = 34$  and  $z_{22} = 72$  ( $i_2 = 2.12$ ) in stage 2. In overrun mode or during braking, the power is reversed from the wheels backwards to the electric machine, which recuperates the power back into the battery storage. The total gear ratio of the serial transmission is  $i_{\text{ges}} = 9.23$ . The transmission is dip lubricated with a gear oil of type “75W-90 API GL-4+”. The service life is 60,000 km according to the manufacturer.

## 4 Test rig set up

The used test rig was developed at the research institute (FZG) for practical tests on BEV transmissions. The test rig is based on the closed power loop principle according to FZG back-to-back test rig [13] consisting of a drive gearbox, test gearbox, torsion shaft, and a load clutch. The principle and design of the test rig are shown in Fig. 2.

The drive and test gearbox have the same gear ratio and correspond to the modified transmission of the Renault Twizy. The drive gearbox is designed as a pure steel gearbox, whereas the test gearbox contains the polymer gears and the steel gears. The load torque is generated by a relative rotation of the torsion shaft and subsequent closing of the load clutch. Due to the closed power loop, the electric motor only has to apply the power dissipation and thus enables efficient testing of BEV transmissions. The test rig offers different lubrication configurations, whereby the modified polymer-steel transmission was tested in anal-

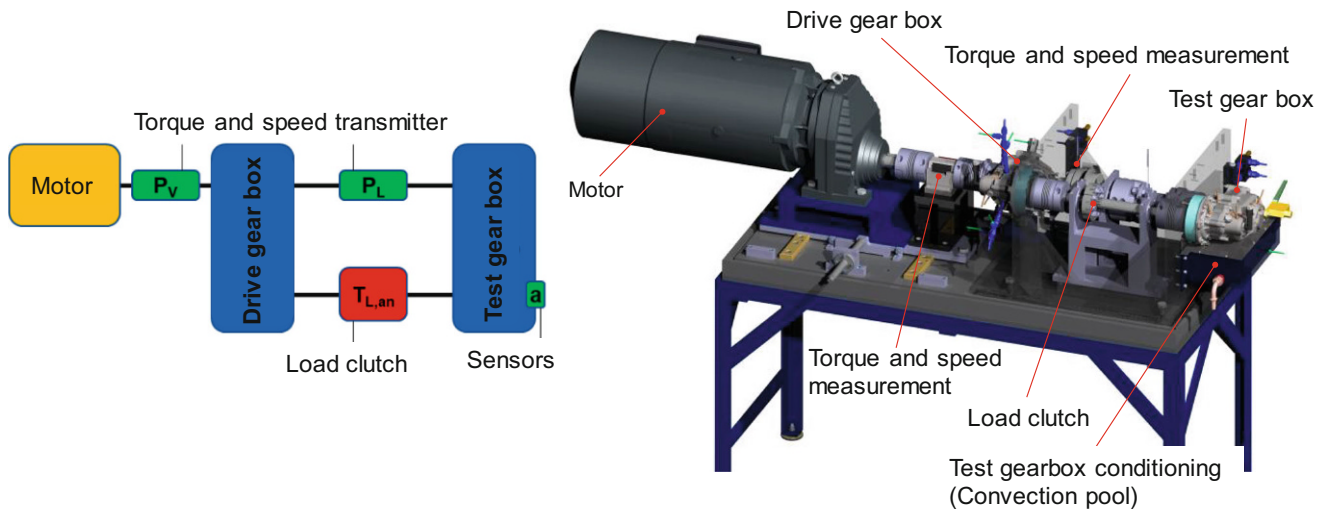


**Fig. 2** Principle and design of the test rig for BEV transmissions

**Table 1** Main gear geometry parameters

		1st stage		2nd stage	
		Polymer pinion	Polymer wheel	Steel pinion	Steel wheel
Normal module $m_n$	mm	2.0		1.5	
Normal pressure angle $\alpha_n$	°	25		20	
Helix angle $\beta$	°	-8	8	15	-15
Number of teeth $z$	-	19	50	32	109
Addendum diameter $d_a$	mm	43.18	104.02	53.60	172.38
Dedendum diameter $d_f$	mm	34.04	95.64	46.69	165.33
Usable root circle diameter $d_{NF}$	mm	36.46	97.91	48.05	167.17
Profile shift coefficient $x$	-	0.20	-0.04	0.31	0.04
Face width $b$	mm	52	50	19	18

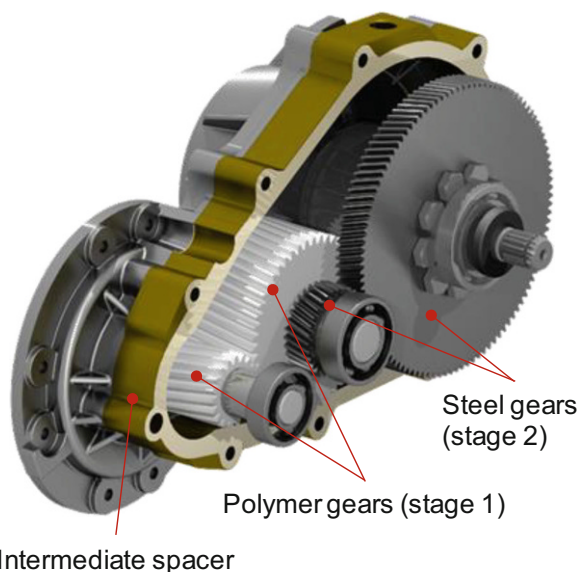


**Fig. 3** Polymer-steel transmission

ogy to its use in the vehicle under dip lubrication. Different operating temperatures can be set using a convection pool for circulating tempered cooling fluid around the gearbox housing. Thermal sensors are mounted inside and around the test gearbox to measure different temperatures (bearings and oil sump temperature) during operation.

## 5 Polymer-steel transmission demonstrator

The development and design of the investigated polymer-steel transmission was mainly carried out in preliminary work (see [4]). It has been shown, that the use of t gears is only possible at the first stage, due to the required torque for the requested driving performance. To enable the use of polymer gears and ensure sufficient load-carrying capacity for the application, the serial transmission was modified in different ways. The critical point in the gear design is the tooth flank pressure at the first stage. The initially planned polymer/steel pairing as replacement, in which the higher stressed pinion would have been made of steel, still re-

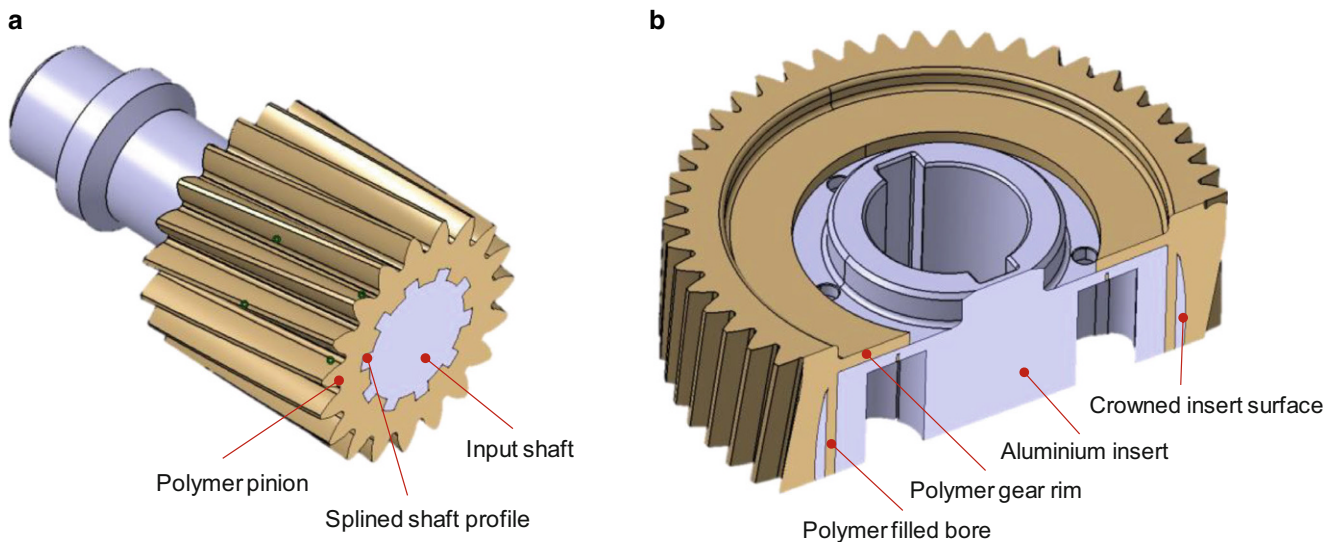


**Fig. 4** Design of the polymer pinion (a) and the wheel (b)

**Table 2** Properties of polymer material [15] for different temperatures

Property	VESTAKEEP® 5000 G ( $\vartheta = 23\text{ }^\circ\text{C}$ )	VESTAKEEP® 5000 G ( $\vartheta = 80\text{ }^\circ\text{C}$ )
Young's modulus in N/mm <sup>2</sup>	3515	3355
Poisson's ratio	0.41	0.41
Density in g/cm <sup>3</sup>	1.30	1.30
Fiber reinforcement	None	

sulted in excessively high flank pressures. Therefore, the first stage is designed as a pure polymer/polymer pairing to further reduce the flank pressure to a tolerable level, due to the soft-soft contact. Moreover, the transmission ratio is somewhat shifted from the first stage to the steel-steel pairing of the second stage considering the available packaging. As a result, it is possible to reduce the tooth forces occurring at the first stage, which has a positive effect on both the tooth root and tooth flank load-carrying capacity. Despite the above steps, it is also necessary to increase the common tooth width of both polymer gears up to  $b=50\text{ mm}$ , in particular, to reduce the flank pressure. The associated increase of the face-width of the gearbox is solved by using a specially designed intermediate spacer, which is placed between the two housing parts. Figure 3 shows the modified transmission with the housing parts and the intermediate spacer. Despite the mentioned modifications, further use of the serial gearbox housing is still possible, due to the unchanged center distances of the two gear stages. The use of polymer gears in the second stage and on the differential is not feasible due to the high load. Both components will therefore continue to be made from a steel material. The experimental investigations were carried out using test gears with a normal module of  $m_n=2.0\text{ mm}$  for the polymer gears and  $m_n=1.5\text{ mm}$  for the steel gears. The detailed

specifications of the test gear geometry of both stages are documented in Table 1. For detailed information on the design of the powertrain and the individual gears, see [4].

The polymer pinion was machined by milling. Therefore, the shaft was first molded with a polymer cylinder, from which the gear teeth were milled afterwards. The input shaft has a splined profile to ensure a sufficiently strong shaft-hub connection by form fit. Instead, the polymer wheel is molded onto an aluminum insert. The aluminum insert is fixed to the gear shaft using a key connection enabling a reliable shaft-hub connection. Holes distributed evenly around the circumference of the aluminum insert are filled with polymer material during the injection molding process and ensure a sufficiently strong form fit between the polymer and the inlay. Additionally, the inlay has a crowning

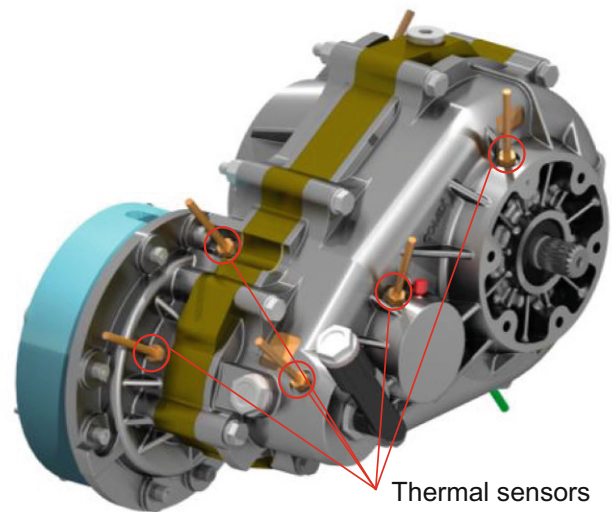


**Fig. 5** Test gear box equipped with thermal sensors

across the tooth width to counteract tooth collapse due to shrinkage. The plastic banding of both inlays with a rim thickness of at least  $t \approx 3 \cdot m_n$  follows the recommendations of ISO 6336 [ISO19a]. Therefore, an influence of the inserts on the load-carrying capacity tests is not suspected. However, lower rim thicknesses can lead to failure of the polymer bandage [14].

As a result of the injection molding process, the polymer gear features a typical tip edge radius acting kind of like a tip relief. A schematic illustration of both gearings is shown in Fig. 4.

The gears of the second stage are machined of case-hardened steel 18CrNiMo7-6 and are designed with a linear tip relief as well as a lengthwise crowning to avoid premature damage caused by meshing interference (for further details on micro geometry see [4]). The steel gears achieve a surface roughness of  $R_a \leq 0.3$  and a tolerance class of  $Q \leq 5$ . As expected, the tolerance class of the polymer gears achieves lower values in the range of  $Q \leq 10$ –12 considering the profile, pitch, and concentricity accuracy. The machined pinion achieves slightly better tolerance classes than the injection-molded wheel ( $Q \leq 10$ ).

It is shown that the determined surface roughness depends strongly on the manufacturing process. Thus, the injection-molded gears achieve an averaged roughness of  $R_a = 0.27 \mu\text{m}$ . However, the roughness of polymer pinions machined in the milling process is higher at  $R_a = 0.42 \mu\text{m}$ . The roughness is measured mechanically in profile direction on three teeth distributed around the circumference. The given values are mean values from several gears. Both polymer gears are made of the non-reinforced high-performance thermoplastic polymer VESTAKEEP® 5000G. The main material properties of VESTAKEEP® 5000G are shown in Table 2 for an ambient temperature of  $\vartheta = 23^\circ\text{C}$  as well as for a relevant operating temperature of  $\vartheta = 80^\circ\text{C}$ .

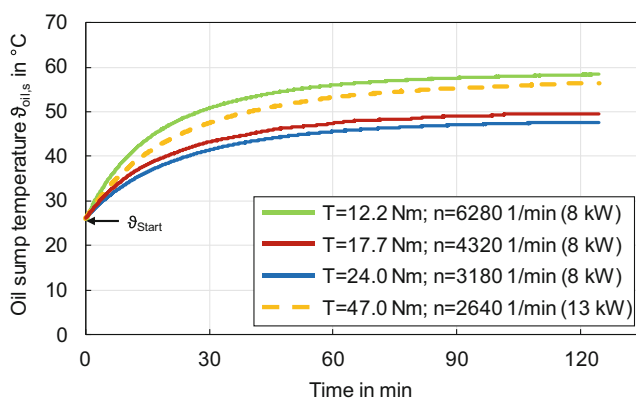


Fig. 6 Oil sump temperature curve at different operating conditions

## 6 Experimental investigations of the load-carrying capacity

To characterize the thermal operating behavior of the modified polymer-steel transmission, experimental investigations on the described test rig were carried out at four various load and speed levels. Three of them were selected on the basis of the load spectrum used in the design process of the gearbox and under consideration of the available continuous power of the e-machine of  $P_{\text{constant}} = 8 \text{ kW}$ . To obtain also information on the thermal behavior under overload, one additional test was conducted at the maximum possible peak power of  $P_{\text{peak}} = 13 \text{ kW}$ . Each operating condition, even peak power, was maintained for approximately 2 h until a stationary temperature was reached. The starting temperature for all tests was the ambient temperature of approx.  $25^\circ\text{C}$  without external heating or cooling of the transmission. To evaluate the thermal operating behavior of the designed polymer-steel transmission, thermal sensors were mounted (see Fig. 5) at different spots on the transmission to monitor the temperature during operation. For evaluating the thermal behavior of the transmission, the oil sump temperature occurring during operation is used, as this is one of the spots where the highest temperatures occur. The oil sump temperature curve for various operating conditions is shown in Fig. 6.

Irrespective of the power transmitted, all temperature curves show a comparable pattern. The temperature in the oil sump rises steadily over a period of 90 min and obtains a constant value after under 2 h of operation. The modified polymer-steel transmission exhibits stable thermal behavior and obtains oil temperatures below  $\vartheta_{\text{oil,s}} \leq 60^\circ\text{C}$  even in continuous operation at maximum peak power. Temperature calculations following VDI 2736 [10] for the polymer gears give tooth temperatures of approx.  $\vartheta_{\text{tooth}} \approx 80^\circ\text{C}$  under these conditions, which is well below the critical temperature range of the used high-performance polymer VESTAKEEP® 5000G. For the design of the polymer gears, strength values for a tooth temperature of  $80^\circ\text{C}$  (see [4]) were also assumed. Thus, it seems to have been a correct assumption based on the test results. Despite the same power input, there is an influence of the different operating conditions. The highest oil temperatures are measured at the lowest load but highest speed. With increasing load and correspondingly lower speed (for constant power), the oil sump temperatures decrease. Compared to the load, this indicates an elevated influence of the speed on the thermal behavior of the modified polymer-steel transmission. This is supported by the oil temperature curve at a peak power of  $P_{\text{peak}} = 13 \text{ kW}$ , where comparable oil temperatures are achieved despite the significantly higher torque. Based on the measured and calculated temperatures, thermal failure of the polymer gears seems unlikely. Signs of thermally

**Fig. 7** Comparison of the tooth contours of the new and actual condition (end of test) of polymer pinion (a) and polymer wheel (b)

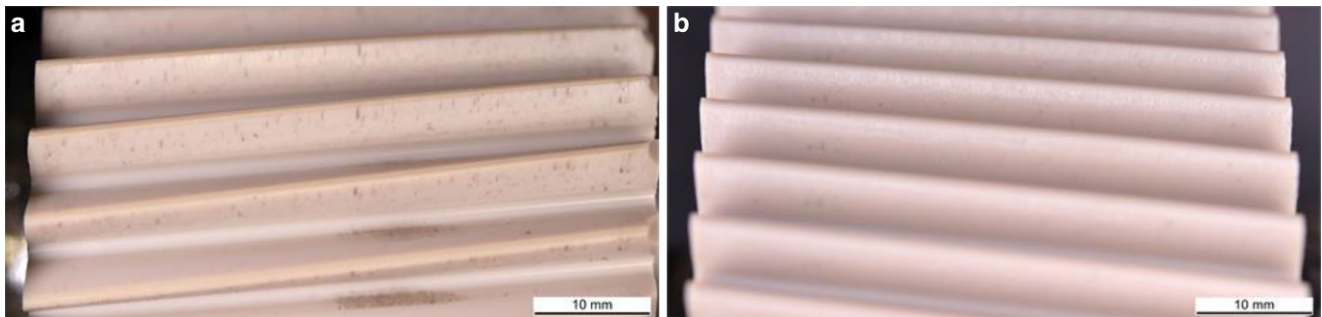
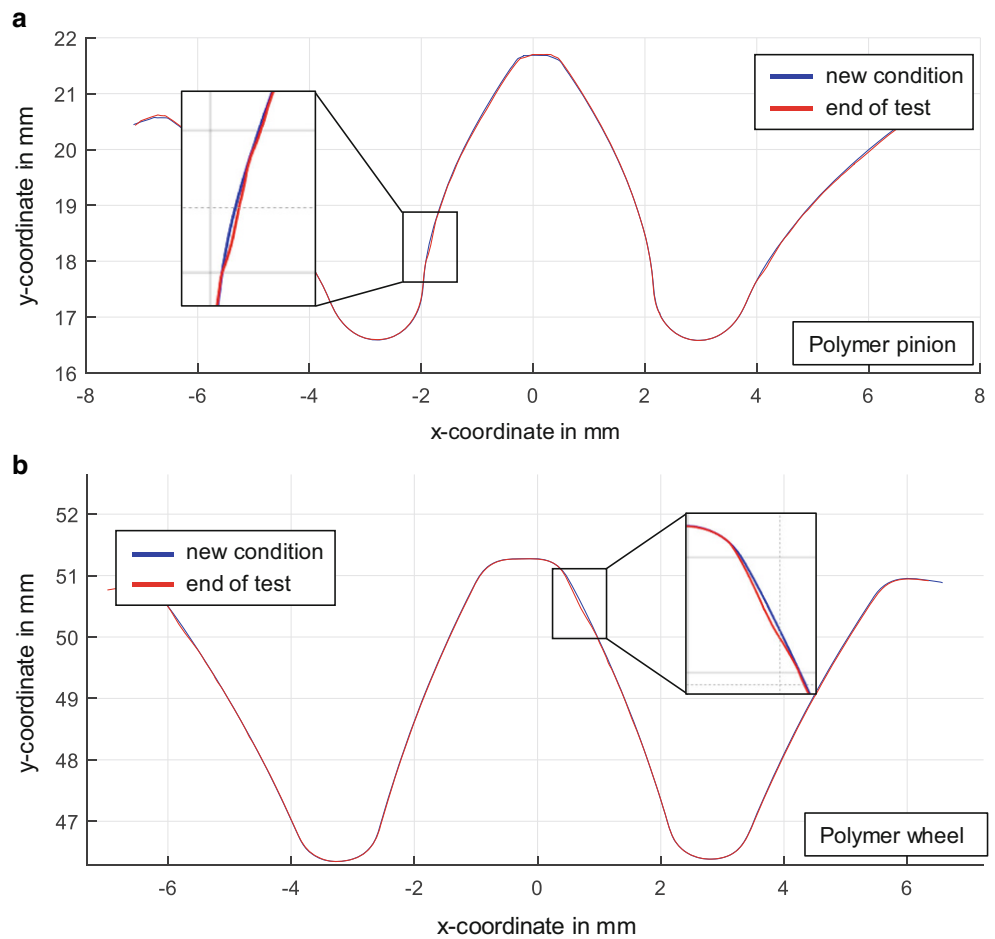


**Fig. 8** Flank condition of the polymer pinion (a) and polymer wheel (b) at end of the test

induced damages, such as melting, were also not detected during the regular inspections.

In further test rig experiments, the load-carrying behavior of the polymer gears was investigated under operating conditions close to the application. The load conditions were selected based on the load spectrum used in the design process. In addition to input torques in the medium load range around  $T_1 = 18 \text{ Nm}$  ( $\sigma_H = 43 \text{ MPa}$ ), which represents the largest proportion of the load spectrum, high load ranges with  $T_2 = 47 \text{ Nm}$  ( $\sigma_H = 69 \text{ MPa}$ ), and  $T_3 = 57 \text{ Nm}$  ( $\sigma_H = 76 \text{ MPa}$ ), at the maximum possible power

of  $P_{\text{peak}} = 13 \text{ kW}$  in continuous operation were also investigated. All three load levels were investigated in sequence according to their proportion in the load spectrum. The theoretical driving distance covered by these tests was over 10,000 km. Within the test period, no damage to the polymer gears was detected causing premature or catastrophic failure of the transmission. As expected, running marks in the form of grooves appeared predominantly on the higher-loaded polymer pinion, particularly after high stresses. However, these signs of wear are not yet considered critical in this condition. Typical wear on the polymer gears as

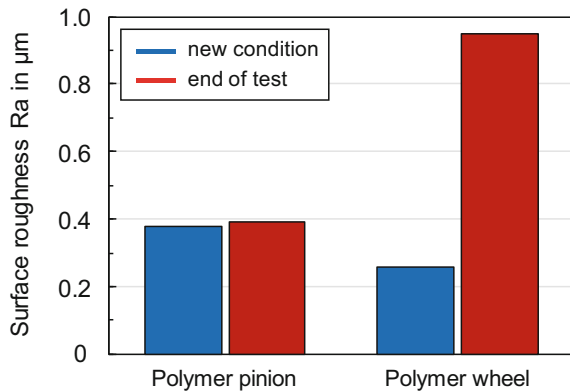


**Fig. 9** Comparison of surface roughness of the new and actual condition of polymer pinion and polymer wheel

a continuous material abrasion cannot be detected. This is in agreement with earlier research work [7, 16, 17] on polymer gears, where the influence of wear under oil lubrication was found to be subordinate. Figure 7 compares the tooth contour measured on a gear measurement machine of the polymer pinion and the polymer wheel in the new condition with the condition after the tests. Slight profile deviations can be seen at the end of the contact line at the usable root circle diameter  $d_{Nf}$  on the polymer pinion. These can also be found at the corresponding area on the tooth tip of the polymer wheel. The reason for this is presumed to be posterior meshing caused by tooth deformation of both polymer gears. As a result of the meshing interference the area around the addendum diameter of the polymer wheel can engage with the dedendum flank area of the polymer pinion with increased pressure peaks in this area leading to localized wear and plastic deformation. This assumption is supported by calculations of the flank pressure (shown in [4]), which show pressure increases in the area of the posterior meshing. Beyond that, no major plastic deformations of the entire teeth could be detected.

In addition, it has been shown that smallest abrasion particles of the steel gears are pressed into the soft polymer tooth flank, which are visible as small black dots and remain there. An impression of the tested tooth flanks of the polymer gears is shown in Fig. 8.

In addition to the previous tests, a mechanically measurement of the surface roughness was carried out on both polymer gears. The comparison of the surface roughness in the new condition with the condition at the end of the test is shown in Fig. 9. There are clear differences in the measured surface roughness between the polymer pinion and the polymer wheel. Whereas the surface roughness of the polymer pinion remains almost unchanged, there is a sharp increase in the surface roughness of the polymer wheel, even though the polymer pinion has endured significantly more load cycles. Effects of the increasing roughness on the polymer

wheel in the form of an increased wear behavior cannot be detected. However, a possible reason for the different roughness behavior may be found in the different manufacturing processes. The polymer pinion was manufactured by machining, whereas the polymer wheel was manufactured by injection molding. As described in [18], there are different material properties between the two manufacturing processes, particularly at the surface. In the injection molding process, an injection molding layer with a higher amorphous microstructure is formed on the tooth surface. In the machining of gears, there is no amorphous surface layer on the tooth flank, but rather a uniform microstructure with a higher crystalline microstructure content. According to [19], the higher proportion of amorphous areas on the tooth flank surface of the injection-molded gears can lead to higher elasticity in the area of the tooth contact and can possible result in a different surface behavior.

Alongside the tests on the test rig, the modified polymer-steel transmission was also mounted in the demonstrator vehicle. Therefore, due to the modifications of the transmission and the associated increase in the package, the demonstrator vehicle requires small modifications as well. The measurement of the acceleration as well as the maximum speed was carried out using the GPS signal of a data logger. The experimental verification under conditions close to the real application of the modified transmission inside the demonstrator vehicle showed no abnormalities. The acceleration behavior as well as the top speed performance basically correspond to that of the serial transmission (see Sect. 2). In terms of noise behavior, no significant difference could be detected compared with the serial steel transmission, either. Overall, on the basis of the measured driving performance and the gained driving impression, the modified polymer-steel transmission achieves comparable performance without restrictions in operation. The condition of the gears after the road tests showed a comparable state like in the test rig investigations. Again, no damages for either the steel or the polymer gears can be detected leading to the assumption that there is sufficient load-carrying capacity of the polymer gears. With regard to the required package space, the new transmission shows a slight increase due to the increased gear width. This is also reflected in the total weight. Due to the modified and additionally required components (e.g. intermediate spacer), the total weight of the new transmission increases slightly from  $m_{\text{serial}} = 10.9 \text{ kg}$  to  $m_{\text{new}} = 11.4 \text{ kg}$ . It should be mentioned that in particular load-carrying capacity was the main priority for the newly designed transmission components, specific weight optimization did not take place for these parts. Generally weight and cost savings were not the focus of this study and are not subject also due to the required framework conditions (use of the same housings, low quantities, ...).

## 7 Conclusion

Polymer gears are increasingly used in applications with higher power transmission. Following this trend, this study designed a polymer-steel transmission for use in a small electric vehicle of the 7Le class. Experimental investigations with focus on the load-carrying capacity of the polymer gears were carried out both on a specially designed test rig as well as in a demonstrator vehicle. Temperature measurements under different operating conditions and long-term operation showed stable thermal behavior for the modified polymer-steel transmission, even at maximum power transmission of  $P_{peak} = 13\text{ kW}$ , with stationary temperatures clearly below the maximum operating temperature of the used high-performance thermoplastic polymer VESTAKEEP® 5000G. As expected, a clear influence of load and speed on the temperature behavior was also noted. Based on the temperatures measured, thermal failure of the polymer gears seems unlikely. In general, no indications of thermally induced damage to the polymer gears were observed. In further load-carrying investigations under operating conditions close to the application, also no damage to the polymer gears was detected leading to premature failure of the transmission. Only some slight but typical running marks appeared on the polymer tooth flanks in the form of grooves, especially after high loads. Minor wear marks could only be detected at the end of the

meshing path on both the polymer pinion and the polymer wheel, presumably due to excessive stresses resulting from posterior meshing. Transferable results are shown by experimental tests in the demonstrator vehicle. The modified polymer-steel transmission achieves a comparable driving performance to the serial transmission made of steel without any premature failure. Therefore, the verification inside the demonstrator vehicle also verifies a sufficient load-carrying capacity of the newly designed polymer gears. Thus, besides the already established typical applications the use of polymer gears appears possible also in fields of increased power transmission, such as for small electric vehicles. In further studies, the full potential of high-performance polymers in terms of cost and weight savings must be exploited while maintaining the load-carrying capacity.

## 8 Nomenclature

The nomenclature is shown in Table 3.

**Acknowledgements** This research project is funded by Zentrales Innovationsprogramm Mittelstand (ZIM-Nr. ZF4810901LL9) of the Bundesministerium für Wirtschaft und Klimaschutz (BMWK). We kindly thank Werner Bauser GmbH (Siemensstr. 2, Wehingen, Germany) for the development and manufacturing of the injection molded test gears and Evonik Operations GmbH (Kirschenallee, Darmstadt, Germany) for the sponsorship and support with material.

**Funding** Open Access funding enabled and organized by Projekt DEAL.

**Conflict of interest** S. Reitschuster, T. Tobie and K. Stahl declare that they have no competing interests.

**Open Access** This article is licensed under a Creative Commons Attribution 4.0 International License, which permits use, sharing, adaptation, distribution and reproduction in any medium or format, as long as you give appropriate credit to the original author(s) and the source, provide a link to the Creative Commons licence, and indicate if changes were made. The images or other third party material in this article are included in the article’s Creative Commons licence, unless indicated otherwise in a credit line to the material. If material is not included in the article’s Creative Commons licence and your intended use is not permitted by statutory regulation or exceeds the permitted use, you will need to obtain permission directly from the copyright holder. To view a copy of this licence, visit <http://creativecommons.org/licenses/by/4.0/>.

## References

1. ISO 6336:2019. Teil 1–5: Calculation of load capacity of spur and helical gears
2. Illenberger CM, Tobie T, Stahl K (2021) Chapter 13: potential and challenges of high performance plastic gears. In: Dudley’s handbook of practical gear design and manufacture. CRC Press, Boca Raton
3. Reitschuster S, Illenberger C, Tobie T, Stahl K (2021) Application of high-performance polymer gears in light urban electric vehicle powertrains. E-Motive 13th Expert Forum Electric Vehicle Drives.

**Table 3** Nomenclature

Symbol	Entity	Description
$b$	$mm$	Face width
$b_w$	$mm$	Common face width
$d$	$mm$	Reference circle diameter
$d_{Nf}$	$mm$	Usable root circle diameter
$F_t$	$N$	Nominal tangential force
$i$	–	Gear ratio
$K_F$	–	Factor for tooth root load
$K_H$	–	Factor for tooth flank loading
$m$	$kg$	Mass
$m_n$	$mm$	Normal module
$u$	–	Gear ratio
$P$	$kW$	Power
$T$	$Nm$	Torque
$Y_{Fa}$	–	Form factor
$Y_{Sa}$	–	Stress correction factor (notch effect)
$Y_{\beta}$	–	Helix angle factor
$Y_{\epsilon}$	–	Contact ratio factor
$Z_E$	$\sqrt{N/mm^2}$	Elasticity factor
$Z_R$	–	Surface roughness factor
$Z_{\beta}$	–	Spiral angle factor
$Z_{\epsilon}$	–	Contact ratio factor
$\sigma_F$	$N/mm^2$	Root stress
$\sigma_H$	$N/mm^2$	Flank pressure at the pitch cylinder

4. Reitschuster S, Illenberger CM, Tobie T, Stahl K (2022) Application of high performance polymer gears in light urban electric vehicle powertrains. *Forsch Ingenieurwes* 86:683–691
5. A review on materials and performance characteristics of polymer gears: Jain, Mohit; Patil, Santosh. *Proceedings of the Institution of Mechanical Engineers, Part C: Journal of Mechanical Engineering Science* 0 (2022)
6. Richtlinie VDI 2736 – Blatt 1:2014. Thermoplastische Zahnräder. Werkstoffe, Werkstoffauswahl, Herstellverfahren, Herstellungsgenauigkeit
7. Hasl C, Illenberger C, Stahl K, Tobie T, Oster P (2018) Potential of oil-lubricated cylindrical plastic gears. *J Adv Mech Des Syst Manuf* 12(1):1–9
8. Maier E, Zieglertrum A, Lohner T, Stahl K (2017) Characterization of TEHL contacts of thermoplastic gears. *Forsch Ingenieurwes* 81:317–324
9. Reitschuster S, Maier E, Lohner T, Stahl K (2020) Friction and temperature behavior of lubricated thermoplastic polymer contacts. *lubricants* 8:67
10. Richtlinie VDI 2736 – Blatt 2:2014. Thermoplastische Zahnräder – Stirnradgetriebe. Tragfähigkeitsberechnung
11. Fürstenberger, M.: Betriebsverhalten verlustoptimierter Kunststoffzahnräder [engl.: Operating behavior of loss-optimized polymer gears], Technische Universität München Dissertation. München 2013
12. Hasl C, Oster P, Tobie T, Stahl K (2017) Bending strength of oil-lubricated cylindrical plastic gears. Modified bending strength calculation based on VDI 2736. *Forsch Ingenieurwes*. <https://doi.org/10.1007/s10010-017-0224-2>
13. DIN 51354:1990. FZG-Zahnrad-Verspannungs-Prüfmaschine
14. Hasl, C.: Zur Zahnfußtragfähigkeit von Kunststoffstirnrädern [engl.: On the tooth root load-carrying capacity of polymer gears], Technische Universität München Dissertation. München 2019
15. Evonik Resource Efficiency GmbH: Product Information: VESTAKEEP® 5000 G. 2011
16. Illenberger C, Tobie T, Stahl K (2021) Operating behavior and performance of oil-lubricated plastic gears. *Forsch Ingenieurwes* 86:557–565
17. Illenberger C, Tobie T, Stahl K (2019) Flank load carrying capacity of oil-lubricated high performance plastic gears—Analysis of the pitting development in back-to-back tests. *International Conference on Gears, Garching*
18. Illenberger, C.: Zahnflankentragfähigkeit ölgeschmierter Kunststoffverzahnungen [engl.: Tooth flank load-carrying capacity of oil-lubricated polymer gears], Technische Universität München Dissertation. München 2022
19. Erhard G (2004) Konstruieren mit Kunststoffen [engl.: Designing with polymers]. Carl Hanser, München, Wien